

## Article

# Advances in the Production of Sustainable Bacterial Nanocellulose from Banana Leaves

David Dáger-López <sup>1</sup>, Óscar Chenché <sup>1</sup>, Rayner Ricaurte-Párraga <sup>1</sup> , Pablo Núñez-Rodríguez <sup>2</sup>,  
Joaquín Morán Bajaña <sup>2</sup> and Manuel Fiallos-Cárdenas <sup>3,\*</sup> 

<sup>1</sup> Facultad de Ciencias e Ingeniería, Universidad Estatal de Milagro, Milagro 091050, Ecuador; ddagerl@unemi.edu.ec (D.D.-L.); ochenchel@unemi.edu.ec (Ó.C.); rricaurtep@unemi.edu.ec (R.R.-P.)

<sup>2</sup> Facultad de Ciencias Agrarias, Campus Milagro, Universidad Agraria del Ecuador, Milagro 091050, Ecuador; pnunez@uagraria.edu.ec (P.N.-R.); jmoran@uagraria.edu.ec (J.M.B.)

<sup>3</sup> Escuela Superior Politécnica del Litoral, ESPOL, Facultad de Ingeniería en Mecánica y Ciencias de la Producción, Campus Gustavo Galindo, Km. 30.5 Vía Perimetral, P.O. Box 09-01-5863, Guayaquil 090902, Ecuador

\* Correspondence: mafiallo@espol.edu.ec

**Abstract:** Interest in bacterial nanocellulose (BNC) has grown due to its purity, mechanical properties, and biological compatibility. To address the need for alternative carbon sources in the industrial production of BNC, this study focuses on banana leaves, discarded during harvesting, as a valuable source. Banana midrib juice, rich in nutrients and reducing sugars, is identified as a potential carbon source. An optimal culture medium was designed using a simplex-centroid mixing design and evaluated in a 10 L bioreactor. Techniques such as Fourier transform infrared spectroscopy (FTIR), scanning electron microscopy (SEM), X-ray diffraction (XRD), and thermogravimetric analysis (TGA) were used to characterize the structural, thermal, and morphological properties of BNC. Banana midrib juice exhibited specific properties, such as pH (5.64), reducing sugars (15.97 g/L), Trolox (45.07  $\mu$ M), °Brix (4.00), and antioxidant activity (71% DPPH). The model achieved a 99.97% R-adjusted yield of 6.82 g BNC/L. Physicochemical analyses revealed distinctive attributes associated with BNC. This approach optimizes BNC production and emphasizes the banana midrib as a circular solution for BNC production, promoting sustainability in banana farming and contributing to the sustainable development goals.

**Keywords:** bacterial nanocellulose; banana leaves; circular bioeconomy; biopolymer; sustainability; simplex-centroid design; fermentation; optimization; yield; biomass



**Citation:** Dáger-López, D.; Chenché, Ó.; Ricaurte-Párraga, R.; Núñez-Rodríguez, P.; Bajaña, J.M.; Fiallos-Cárdenas, M. Advances in the Production of Sustainable Bacterial Nanocellulose from Banana Leaves. *Polymers* **2024**, *16*, 1157. <https://doi.org/10.3390/polym16081157>

Academic Editors: Abdel-Hamid I. Mourad and Bruno Medronho

Received: 22 January 2024

Revised: 16 March 2024

Accepted: 18 March 2024

Published: 20 April 2024



**Copyright:** © 2024 by the authors. Licensee MDPI, Basel, Switzerland. This article is an open access article distributed under the terms and conditions of the Creative Commons Attribution (CC BY) license (<https://creativecommons.org/licenses/by/4.0/>).

## 1. Introduction

Cellulose is a biopolymer with a high molecular weight, composed of glucose units linked by  $\beta$ -1,4-glycosidic bonds [1]. The molecular formula of cellulose is  $(C_6H_{10}O_5)_n$ , where 'n' represents the number of linked glucose units that comprise the polymer chain. It serves as the primary component of plant biomass, derived from sources such as plants and wood [2]. Various organisms, including green algae (*Valonia*) and microorganisms, such as Gram-negative bacterial species like *Acetobacter* and *Agrobacterium* [1,3–6], as well as Gram-positive bacteria like *Lactobacillus* [5], participate in cellulose synthesis. This particular form of cellulose is referred to as bacterial cellulose (BC) or bacterial nanocellulose (BNC). The Gram-negative bacterium *Gluconacetobacter xylinus*, formerly known as *Acetobacter xylinum*, stands out as the predominant producer of BNC [3,7].

Plant cellulose and BNC exhibit both similarities and differences in structure and properties. Both are celluloses with a similar chemical structure [8]. However, BNC is characterized by higher crystallinity and a greater degree of polymerization compared to plant cellulose, imparting superior strength and elasticity [4,9]. Additionally, the crystalline structure of BNC contains nanostructures that form a network of microfibrils and macrofibrils,

resulting in a high water absorption capacity and improved mechanical stability [10]. Furthermore, it is characterized by a more homogeneous nanostructure, primarily composed of I $\alpha$  and I $\beta$  allomorphs [4,11,12]. The structure of BNC may vary depending on its origin and extraction method. This biopolymer lacks lignin, hemicelluloses, and pectin, which are typically present in cellulose derived from plants [11–14]. It is noteworthy that the cost of BNC production is typically higher than that of the plant cellulose process [13,15,16].

Cellulose can be produced through two main strategies: chemical synthesis and biochemical synthesis (fermentation). In the chemical synthesis process, it unfolds in two phases. Initially, the isolation and purification of cellulose from lignocellulosic biomass (LB) are performed using mechanical and chemical methods. During this stage, the LB undergoes physical treatments to reduce its size, followed by an intensive chemical treatment involving pulping and bleaching with sodium hydroxide (NaOH) and sodium sulfide (Na<sub>2</sub>S), followed by an additional bleaching stage with chlorine dioxide (ClO<sub>2</sub>) [17]. In the second phase, mechanical homogenization or acid hydrolysis is carried out to produce cellulose nanofibers (CNF) and cellulose nanocrystals (CNC), respectively [18]. The cellulose content can be affected by the pulping or alkaline bleaching process, resulting in a decrease in cellulose yield [19–21]. This situation implies the need for the costly recovery of other components present in the lignocellulosic biomass (LB), such as hemicellulose and lignin, found in black liquor pulp [22,23]. Additionally, the production of CNF or CNC presents economic and environmental challenges due to high energy consumption and the use of corrosive mineral acids, leading to the generation of acidic waste [13].

On the other hand, the fermentation or biochemical synthesis methodology is a bottom-up approach. Microorganisms utilize various compounds present in the biomass, such as monosaccharides and nitrogen compounds, to produce diverse products of industrial interest [3,10,24,25]. This process encompasses physical processes [26], as well as chemical and biological treatments to primarily extract sugars from lignocellulosic biomass [8,27–29]. Certain bacteria can synthesize BNC by secreting it in the outer membrane of their cells [30–32]. Glucan chains are first synthesized in the inner membrane and then secreted to form nano-sized protofibrils (2–4 nm). These protofibrils tightly aggregate to form BNC fibers with a diameter of 20–100 nm [6,13,22]. BNC synthesis is more efficient in the purification and extraction of cellulose compared to vegetable cellulose, as it is produced without lignin and other associated impurities [9,15,32]. BNC has gained popularity due to its simple production process, non-toxicity, high purity, biocompatibility, and environmental friendliness [31,33]. BNC can be obtained from various types of biomasses through sustainable strategies, such as the production of kombucha tea. This beverage is fermented using a symbiotic culture of yeast and bacteria (SCOBY) [34,35]. It can also be obtained in the production of a dessert known as ‘coconut cream’ [36,37].

Figure 1 illustrates the various techniques employed in the production of bacterial cellulose (BC) using different carbon sources. At the biomass level, the following two main categories can be identified: (i) residual biomass (RB), encompassing industrial wastewater and food waste, among others; and (ii) lignocellulosic residual biomass (LRB), primarily composed of rigidly assembled cellulose, hemicellulose, and lignin [38–40]. It should be noted that, under certain circumstances, LRB may contain oil, starch, proteins, and juices [41]. These juices may contain reducing sugars (RS) used as a carbon source in fermentation processes [25,26]. In cases where LRB does not contain RS-rich juices, several procedures, such as physical pre-treatment, chemical hydrolysis, or enzymatic hydrolysis, are necessary. The aim of these methods is to expedite the production of cellulose-derived sugars to serve as carbon sources for BNC production [27]. It is crucial to recognize that globally, the availability of waste biomass presents substantial potential for use in sustainable and environmentally friendly production opportunities [3]. In addition to the carbon sources mentioned above, processed substrates such as sucrose or glucose can also be used. Glucose is frequently used as a reagent in laboratory conditions, employing the Hestrin-Schramm (HS) culture technique, which is widely recognized for its efficacy in the

production of BNC [42,43]. Processed sugar is commonly used as a carbon source for the production of fermented kombucha tea [44].

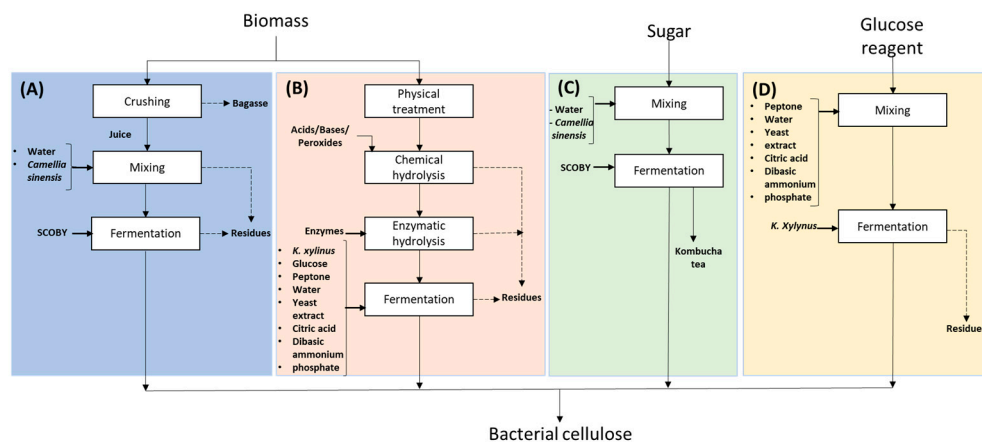


**Figure 1.** Different approaches for obtaining bacterial cellulose using different carbon sources. (A) Residual biomass rich in sugary juices, which requires minimal physical treatments to extract its sugars, which are then used as a carbon source. (B) Residual biomass containing sugars requires physical, chemical, or biological pre-treatment to extract the sugars. These sugars are then used as a carbon source in fermentation processes. (C) Kombucha tea production uses conventional sugar (sucrose). (D) The carbon source in Hestrin-Schramm (HS) medium is reagent-grade glucose.

BNC stands out as a highly promising natural polymer in scientific research [3]. Its nanostructure and exceptional properties render it a valuable biomaterial with diverse applications [30]. Moreover, BNC exhibits potential as a sustainable alternative to petrochemicals in various industrial applications owing to its remarkable properties [13]. In the biomedical field, researchers have synthesized wound dressing membranes composed of BNC, incorporating antimicrobial plant extracts through the ex situ incorporation technique [45]. Furthermore, investigations have demonstrated that BNC films, enriched with antibiotics such as amoxiclav and fluconazole, effectively serve as antibacterial and antifungal materials, contributing to wound healing [4]. However, the scope of BNC transcends the biomedical realm. Its applicability has been explored in the paper manufacturing industry, where it has been studied as a reinforcing agent [46]. Despite the advantages BNC offers over plant cellulose, its production process incurs significant costs. To address this, research has been directed towards the potential utilization of industrial and agricultural waste, including spent brewer's yeast, acid by-products from alcohol production, sugar beet molasses, whey, sucrose, acid hydrolysate from potato peel waste, coconut husks, and banana leaves [47]. In an effort to enhance efficiency and reduce production costs associated with BNC, various studies have been conducted [26,48–51].

During banana cultivation, diverse lignocellulosic residues are generated, including the banana leaf (BL), which contains a juice lodged in the midrib and is enriched with nutrients and reducing sugars. Frequently, this residual biomass is left to decompose in agricultural soil, posing potential environmental and health hazards [52]. To date, there remains a substantial lack of characterization regarding the physical and chemical properties of banana midrib juice (BMJ). Nevertheless, studies have demonstrated the efficacy of BMJ in bioethanol production [25] and bacterial cellulose generation [26]. Furthermore, no investigations have yet focused on optimizing the process for obtaining BNC from BMJ.

Experimental design (DoE), particularly in its mixture designs (MDs) modality, constitutes a valuable resource for optimizing procedures and product design in various domains [53,54]. Through the use of DoE, researchers have the ability to explore multiple process parameter configurations with the aim of optimizing product quality and reducing costs [55–58]. Considering the successes achieved by MDs in improving processing conditions and developing novel products [59–61], there is a potential application for their

adoption in the manufacturing of various products [56,62]. Based on mixture experiments, some modified mixture design methods have been developed, including the simplex-centroid design method. This design method is commonly applied in the formulation of industrial products such as food processing, chemical formulations, material design, textile fibers, and pharmaceutical drugs [62–64]. However, to date, specific information regarding the implementation of the simplex-centroid mixture design in the BNC generation process is lacking.

This study aimed to achieve several objectives: firstly, to analyze the physicochemical properties of both BMJ and the components used in the fermentation medium, such as green tea infusion (GTI) and SCOBY. Subsequently, it aimed to assess the composition of SCOBY through metagenomic techniques. Thirdly, the simplex-centroid mixture design (SCMD) was employed to identify the optimal combination of culture media to maximize the yield in BNC production from BMJ. Lastly, the information gathered from the SCMD was utilized to scale up production to a 10 L reactor, followed by a detailed assessment of the physical and chemical properties of the obtained BNC.

## 2. Materials and Methods

The initial part of this section provides a detailed overview of the procedures employed to analyze the physical and chemical properties of BMJ, GTI, and SCOBY. Following this, the experimental design based on the simplex-centroid methodology and its validation concerning the scalability of production to a 10 L capacity are delineated. Moreover, it includes a description of the methods used to assess the physical and chemical properties of the BNC obtained in the scaled-up medium.

### 2.1. Materials

Banana leaves were gathered from a conventional plantation of Cavendish subgroup bananas (*Musa acuminata*) situated in Milagro city, Guayas province, Ecuador. The protocol outlined by [26] was followed to extract and process the BMJ. This process involved pasteurizing the BMJ at 121 °C for 15 min. The pasteurized BMJ resulting from the experiment was stored in amber glass jars at a constant temperature of 4 °C for subsequent analysis. The green tea utilized in this research was procured from a local tea processing company and prepared using conventional methods. The GTI was prepared by immersing bagged green tea, employing a ratio of 10 g of green tea leaves per liter, into distilled water heated to 95 °C. The tea steeped for 5 min, after which the bags were removed, and the infusion was kept at 37 °C in a water bath (NTT-20S; Eyela, Tokyo, Japan) until it was employed in formulating various fermentation media and subsequent analyses. SCOBY originated in the microbiology laboratory at the State University of Milagro. It encompasses strains of *Komagataeibacter hansenii* ATCC 23769, *Brettanomyces bruxellensis*, and *Brettanomyces anomalus*.

### 2.2. Analysis of the Physical and Chemical Properties of Banana Midrib Juice, Green Tea Infusion, and SCOBY

The analytical procedures conducted in the BMJ following pasteurization, GTI, and SCOBY are detailed below. The density of the solutions was determined using a pycnometer at 25 °C. Acidity measurements were performed using a digital pH meter (APERA Instruments, LLC-PC60, USA, Columbus, OH, USA), previously calibrated to pH values of 4.0 and 7.0. The concentration of total soluble solids (°Brix) in the JNB at 25 ± 2 °C was assessed using a digital refractometer (Atago Co., Ltd., Tokyo, Japan). To analyze reducing sugars, the 3,5-dinitrosalicylic acid method was employed, quantifying the concentration of reducing sugars using the standard curve of D-glucose [65]. Electrical conductivity was determined using a portable multimeter (HACH-HQ40D, Loveland, CO, USA).

The chromatic profile was assessed using the CIELAB system, involving the measurement of three parameters: L\*, a\*, and b\*. The L\* parameter reflects luminosity (ranging from 0 for black to 100 for white), while a\* and b\* indicate chromatic variations between

green/red and blue/yellow hues, respectively. A Konica Minolta CR5 benchtop colorimeter (Tokyo, Japan) was employed for these measurements.

To assess the antioxidant capacity, the DPPH radical scavenging assay was performed with minor adaptations [66]. A mixture of 100  $\mu\text{L}$  of the sample and 1.9 mL of a DPPH radical solution diluted in methanol in a 1:1 ratio was prepared. After 30 min at room temperature and in darkness (23–26  $^{\circ}\text{C}$ ), the free radical scavenging capacity was evaluated by measuring the absorbance at 517 nm. Results were expressed as mean percentages of inhibition and were conducted in triplicate to ensure data reliability.

### 2.3. Experimental Design for Bacterial Nanocellulose Production

The response surface methodology employed a simplex-centroid mixing experimental design to formulate the medium. This design considers  $2^q - 1$  combinations of mixtures, where  $q$  represents the number of components of the system, namely the BMJ, GTI, and SCOBY. The factors represent the fraction of each raw material in the mixture, ranging from 0 to 1, with no restrictions on the design space.

The feasible space for a three-component mixture experiment is defined as a simplex, which is a triangle. The composition of each mixture varies based on its position in this region. The vertices of the simplex represent pure mixtures, which are composed of 100% of a single ingredient [45,50].

The mathematical model used is as follows:

$$Y = \sum_{1 \leq i \leq q} \beta_i x_i + \sum_{1 \leq i < j \leq q} \beta_{ij} x_i x_j + \sum \beta_{123} x_1 x_2 x_3 \quad (1)$$

where  $Y$  represents the dependent variable, bacterial nanocellulose yield during the 14-day fermentation period;  $x_1$ ,  $x_2$ , and  $x_3$  correspond to the independent variables BMJ, GTI, and SCOBY, respectively. Model adequacy was evaluated by examining the  $R^2$ ,  $R^2$ -adjusted, and  $p$ -value. The modeling and optimization were carried out using the MIXEXP library in RStudio software (version 4.0.3).

### Culture Medium Optimization

During the initial stage, experiments were conducted in 500 mL wide-mouth glass bottles containing 100 mL of culture medium under aerobic conditions. To maintain optimal conditions, the flasks were covered with sterile paper to prevent light exposure and incubated at a constant temperature of 30  $^{\circ}\text{C}$  for 14 days. At the end of this period, BNC films were collected from the surface of the culture medium. The collected films underwent a thorough washing process to eliminate bacterial cells using a 0.4 N NaOH solution at 80  $^{\circ}\text{C}$ , followed by rinsing with distilled water until achieving a neutral pH. All experiments were conducted in triplicate to ensure result reproducibility. The purified BNC films were freeze-dried at  $-80$   $^{\circ}\text{C}$  for 24 h and weighed ( $Wd$ ). The study analyzed the yields of BNC film production, calculated using Equation (2) provided by Ref. [67].

$$\text{CN production yield (\%)} = \frac{Wd}{V(So - Sf)} \times 100 \quad (2)$$

where  $Wd$  is the mass of BNC produced (g),  $V$  is the reaction volume (L),  $So$  is the initial substrate concentration in the medium (g/L), and  $Sf$  is the final substrate concentration in the medium (g/L).

### 2.4. Production of Bacterial Nanocellulose Using Optimal Values

The optimal values obtained were utilized to scale up the production process to 10 L of medium under static conditions at 30  $^{\circ}\text{C}$ . The pH, turbidity, and BNC yield on a dry basis were assessed at various time points (0, 4, 7, and 14 days).

Additionally, the physicochemical properties of the NCB were evaluated using techniques such as scanning electron microscopy (SEM), Fourier transform infrared spectroscopy (FTIR), thermogravimetric analysis (TGA), and X-ray diffraction (XRD).

#### 2.4.1. Scanning Electron Microscopy

Following the fermentation phase, the BNC underwent treatment with NaOH and distilled water, followed by a drying process through freeze-drying at  $-80\text{ }^{\circ}\text{C}$  using the 4.5 L FreeZone<sup>®</sup> system (Labconco, Kansas City, MO, USA). Subsequently, morphological analysis of the BNC was conducted using an FEI<sup>®</sup> Inspect S SEM scanning electron microscope (FEI Company, Hillsboro, OR, USA). During the preparation of the SEM images, the dried BNC was fixed and coated with a thin layer of gold nanoparticles. The experiments were performed at a magnification of  $10,000\times$  and an accelerating voltage of 14.5 kV.

#### 2.4.2. Fourier Transform Infrared Spectroscopy

The chemical structure of the dry BNC was determined using FTIR. Spectra were recorded using the attenuated total reflectance (ATR) technique on a Spectrum GX spectrometer (PerkinElmer, Waltham, MA, USA) in the range of  $4000$  to  $500\text{ cm}^{-1}$ . A total of 32 spectra were accumulated with a resolution of  $4\text{ cm}^{-1}$ . The spectral data were normalized and subjected to background and baseline corrections. Subsequently, graphical representations were generated using OriginPro 9.0 software (OriginLab Corporation, Northampton, MA, USA).

#### 2.4.3. Thermogravimetric Analysis

The thermal stability of BNC was determined by conducting TGA using a TA<sup>®</sup> Instruments Q-600 with a simultaneous DTA thermal analyzer. The BNC samples were weighed and placed in a tray with a weight range of 2 to 5 mg. The samples were heated with nitrogen from  $25\text{ }^{\circ}\text{C}$  to  $1000\text{ }^{\circ}\text{C}$  at a constant heating rate of  $10\text{ }^{\circ}\text{C}/\text{min}$ .

#### 2.4.4. X-ray Diffraction

The dried BNC was ground to a powder for X-ray diffraction analysis. The sample was analyzed with nickel-filtered Cu-K $\alpha$  radiation ( $\lambda = 0.15418\text{ nm}$ ). Diffraction maps were recorded at room temperature using a PANalytical<sup>®</sup> X-ray diffractometer X'Pert, operating at 45 kV and 40 mA. The  $2\theta$  range was from  $5$  to  $80^{\circ}$ , with a scanning speed of  $0.01^{\circ}/\text{s}$ . The crystallinity index (*CrI*) of the BCs was determined using Segal's technique [68], as shown in Equation (3):

$$CrI (\%) = (I_{200} - I_{am}) / (I_{200}) \times 100\% \quad (3)$$

Here, *CrI* represents the crystallinity index,  $I_{am}$  represents the minimum diffraction intensity at around  $2\theta = 18^{\circ}$ , and  $I_{200}$  is the maximum diffraction intensity of (002) lattice diffraction at around  $2\theta = 22.6^{\circ}$  [69].

### 3. Results and Discussion

#### 3.1. Physical and Chemical Characteristics of the Components Utilized in the Preparation of the Culture Medium

In the context of this research, a meticulous analysis of the physicochemical properties inherent to the components of the culture medium formulation has been carried out. The results derived from these evaluations can be found in Table 1.

pH plays a pivotal role in fermentation processes. BMJ exhibited a less acidic nature in comparison to GTI and SCOBY. Nonetheless, Ref. [25] reported a pH of 6.8 for BMJ, whereas Ref. [70] observed a pH of  $6.4 \pm 0.15$  for banana leaf biomass. The observed variability in the pH of JNB may be attributed to factors such as soil type, genetic variability, and the application of chemical fertilizers [67,71]. On the other hand, the pH value of GTI closely aligns with findings from previous studies [72–74]. The acidity of GTI may be attributed to the extraction of compounds inherent in tea leaves, including organic acids, phenols, carboxylic groups, and amino acids [74]. The pH of SCOBY exhibits analogous values to those documented in other studies [75,76]. It has been postulated that maintaining an acidic pH range, typically ranging from 6 to 3, may foster the proliferation of a broader spectrum of microorganisms, potentially enhancing bacterial nanocellulose production [26].

**Table 1.** Physicochemical properties of individual components in formulation.

Parameters	BMJ	GTI	SCOBY
pH	5.64 ± 0.02	5.37 ± 0.02	3.20 ± 0.02
Density (g/mL)	1.02 ± 5.0 × 10 <sup>-3</sup>	1.01 ± 5.0 × 10 <sup>-3</sup>	1.05 ± 5.0 × 10 <sup>-3</sup>
°Brix	4.000 ± 0.32	1.33 ± 0.32	12.83 ± 0.32
Reducing sugars (g/L)	15.97 ± 0.49	0.00 ± 0.00	5.67 ± 0.49
Conductivity (μS/cm)	16.57 ± 5.70 <sup>a</sup>	39.40 ± 5.70 <sup>a</sup>	75.13 ± 5.70
Antioxidant activity (DPPH) (%)	71.00 ± 0.11	70.27 ± 0.11	16.18 ± 0.11
Trolox (μM)	45.07 ± 0.58 <sup>b</sup>	45.47 ± 0.58 <sup>b</sup>	8.17 ± 0.58
L*	27.55 ± 0.13	92.23 ± 0.13	90.97 ± 0.13
a*	0.49 ± 0.15	-5.24 ± 0.15	-0.42 ± 0.15
b*	-0.35 ± 0.32	34.48 ± 0.32	15.33 ± 0.32
chroma	0.62 ± 0.16	27.43 ± 0.16	15.13 ± 0.16
Hue	324.03 ± 0.32	210.33 ± 0.32	90.50 ± 0.32

BMJ: banana midrib juice; GTI: green tea infusion; SCOBY: Symbiotic Colony Of Bacteria and Yeast. Means of the three replicates ± standard deviation. The same superscript letters within a row indicate that there are no significant differences ( $p \leq 0.05$  according to the significant differences ( $p \leq 0.05$  according to Tukey's test).

The determination of total soluble solids (TSS) concentration can be achieved through density and Brix measurements. The TSS values observed in GTI align consistently with those reported in prior investigations [74]. As posited by [73], the presence of phenolic compounds, alkaloids, carbohydrates, amino acids, pigments, vitamins, and other minor compounds contributes to the TSS in GTI. SCOBY exhibits a higher density and °Brix, indicative of a heightened concentration of soluble compounds compared to BMJ and GTI. This elevated concentration may potentially provide a richer nutrient milieu for microbial activity during the fermentation process.

In comparison to GTI and SCOBY, BMJ had the highest amount of reducing sugars. According to [77], the banana cultivars Williams and Grand Nain had a total soluble carbohydrate content of  $25.21 \pm 2.84$  and  $23.50 \pm 0.86$  mg/g, respectively. Similarly, Ref. [25] found that the pressed juice of banana leaves contained a total sugar of 14%, with glucose (18.9 g/L), sucrose (13.29 g/L), and fructose (15.63 g/L) present. It should be noted that banana composition can be significantly influenced by factors such as soil type and genetic variability [71,77].

The electrical conductivity of BMJ suggests a remarkable presence of ions in this solution. Ref. [70] determined that the conductivity of banana leaf biomass was  $1.98 \pm 0.02$  mS/cm, a higher value than reported in this research. According to [25], the juice obtained by pressing banana leaves possesses a significant amount of macroelements (K, Na, and Mg) and traces of microelements (Fe, Cu, Zn, and B). Regarding GTI, Ref. [72] determined three major elements (Ca, K, and Mg) and eleven trace elements (Al, As, B, Cd, Co, Cr, Fe, Mn, Pb, Se, and Zn) in green tea leaves. The findings suggest the absence of significant differences in electrical conductivity between BMJ and GTI, possibly attributable to similarities in ionic composition, indicating uniformity in electrical properties. Ref. [78] indicates that the presence of these macroelements (K, Na, and Mg) and microelements (Fe, Cu, Zn, and B) in the culture medium is considered crucial in microbial fermentation, indicating that they have a significant effect on yeast growth rate, substrate consumption, and fermented beverage production yield.

On the other hand, BMJ exhibits a remarkable antioxidant capacity of 71.0%, along with a significant concentration of Trolox, highlighting its efficacy in protecting against oxidative damage. Phytochemicals, such as flavonoids, tannins, and terpenoids, are present in banana leaves [79]. Similarly, GTI also demonstrates high antioxidant activity, attributed to the phytochemicals found in green tea. Ref. [74] reported comparable values of 76.71–95.48% inhibition. This capability may provide protection against oxidative damage during fermentation. The results revealed no significant difference in Trolox concentration (μM) between BMJ and GTI. This finding could be attributed to the possible similarity in antioxidant composition.

The colorimetric parameters L\*, a\*, and b\* offer detailed insights into the luminosity, reddish or greenish tones, and yellow or blue hues present in the analyzed materials. In the case of BMJ, the luminosity value indicates a relatively subdued light shade. The values of a\*

and  $b^*$  suggest a minimal tendency towards reddish tones and a slight inclination towards blue tones. In contrast, GTI has a higher  $L^*$  value, indicating greater brightness or clarity compared to BMJ. However, the  $a^*$  and  $b^*$  values suggest a tendency towards greenish and bluish tones. These results align with previous studies [72,74]. Ref. [72] proposes that  $a^*$  and  $b^*$  values in GTI are closely linked to elevated Total Dissolved Solids (TDS) and pH, noting that an increase in TDS can intensify the green tea's color. It is essential to understand the relationship between color attributes and the chemical composition of the product to comprehend the influence of media components on the final product's visual characteristics. However, the SCOBY has the highest brightness value, indicating greater visual clarity. Additionally, the  $a^*$  and  $b^*$  values suggest a tendency towards reddish and yellowish tones.

The chroma values, representing color saturation, vary significantly among samples. BMJ exhibits the lowest chroma value, indicating lower color saturation. Meanwhile, GTI and SCOBY show significantly higher values, suggesting greater saturation and vibrancy in the hues present in these samples. Brewing water is a key factor influencing tea brew color. Results from the analysis of  $L^*$ ,  $a^*$ ,  $b^*$ , chroma ( $C^*$ ), and hue ( $H^*$ ) values of BMJ, GTI, and SCOBY samples indicate significant differences in their color characteristics. The SCOBY sample is the brightest, reddest, and yellowest of the three, while the BMJ sample is the darkest, greenest, and least saturated. Such variations could be related to the presence and concentration of biochemical compounds, such as phytochemicals or antioxidants, influencing their visual characteristics and potentially their functional properties in fermentation and biological production applications.

### 3.2. Optimized Culture Medium Using Simplex-Centroid Design

The study utilized a simplex-centroid design to assess the effect of three variables: BMJ, GTI, and SCOBY inoculation, on the optimal yield of bacterial nanocellulose. Table 2 provides detailed information on the experimental design, which generated nine different combinations.

**Table 2.** Design of a simplex-centroid mixture with three components to obtain bacterial nanocellulose.

Treatment	BMJ	GTI	SCOBY	Yield (g L <sup>-1</sup> )
1	1	0	0	4.17 ± 0.10
2	0	1	0	3.25 ± 0.08
3	0	0	1	4.13 ± 0.12
4	0.5	0.5	0	4.75 ± 0.15
5	0.5	0	0.5	6.17 ± 0.11
6	0	0.5	0.5	5.12 ± 0.09
7	0.33	0.33	0.33	7.13 ± 0.05
8	0.33	0.33	0.33	7.10 ± 0.10
9	0.33	0.33	0.33	6.94 ± 0.13

BMJ: banana midrib juice; GTI: green tea infusion; SCOBY: Symbiotic Colony Of Bacteria and Yeast.

The response variables were analyzed using analysis of variance (ANOVA) to select a suitable model. ANOVA was chosen based on several measured criteria, with a 95% confidence interval, as presented in Table 3. The use of ANOVA allowed for the analysis of the influence of each combination, with a significance level of 0.05. The RStudio statistical package MIXEXP was used to perform this analysis.

The study found that the BMJ, GTI, and SCOBY components had a significant impact on BNC procurement performance ( $p$ -value < 0.05). Additionally, the mixing ratios of  $x_1x_3$ ,  $x_2x_3$ , and  $x_1x_2x_3$  also had a significant effect. However, the  $x_1x_2$  combination did not significantly affect the yield of bacterial cellulose production ( $p$ -value > 0.05).

**Table 3.** Regression analysis for bacterial nanocellulose production.

Factors	Coefficient	Std. Error	t-Value	p-Value	
$x_1$	4.170	0.1018	40.973	<0.001	Very Significant
$x_2$	3.250	0.1018	31.933	<0.001	Very Significant
$x_3$	4.130	0.1018	40.580	<0.001	Very Significant
$x_1:x_2$	4.160	0.4986	8.344	<0.05	Low Significant
$x_1:x_3$	8.080	0.4986	16.206	<0.01	Significant
$x_2:x_3$	5.720	0.4986	11.472	<0.01	Significant
$x_1:x_2:x_3$	32.722	2.6968	12.133	<0.01	Significant

A regression analysis was conducted on the mixture variables (BMJ, GTI, and SCOBY), revealing that their relationships could be statistically modeled. The model's performance was assessed using the  $R^2$  coefficient. According to existing literature, the coefficient of determination ( $R^2$ ) indicates conformity when surpassing 70% and is further interpreted favorably as it approaches 1.00, signifying a superior fit of the model to real data or its overall significance [80]. Additionally, the adjusted  $R^2$  was employed to evaluate the alignment of experimental results with theoretical outcomes [81]. In this context,  $p$ -values were less than 0.05, and both coefficients of determination ( $R^2$  and adjusted  $R^2$ ) reached 99.99% and 99.97%, respectively. The F-statistic, registering at 3.879 with a  $p$ -value of 0.0002578, underscores the overall significance of the model. The residual standard error, standing at 0.1018 with 2 degrees of freedom, emphasizes its close agreement with the obtained data. Furthermore, the test for lack of fit, with a  $p$ -value greater than 0.05, indicated that the model was sufficient to predict BNC production performance. See Equation (4).

$$\begin{aligned} \text{Yield} = & 4.170x_1 + 3.250x_2 + 4.130x_3 + 4.160x_1 \times x_2 + 8.080x_1 \times x_3 \\ & + 5.720x_2 \times x_3 + 32.722x_1 \times x_2 \times x_3 \end{aligned} \quad (4)$$

Statistical analysis shows that all three factors have a significant influence on bacterial nanocellulose production. The regression coefficients for each factor are positive, indicating that an increase in any of them correlates with an increase in bacterial nanocellulose production. The model without an intercept is obtained by removing the constant term from the model with an intercept. When all factors are at zero, the yield of bacterial nanocellulose production is considered to be zero.

The mixing contour plot within the CSD visually represents the impact of variables on BNC production. It uses color coding to differentiate between different levels of performance. Figure 2 exemplifies this representation, where darker shades of red indicate lower performance, while lighter shades and yellow indicate gradual improvement and areas of higher performance, respectively. It is worth noting that a composition closer to the central point leads to a significant increase in the yield of BNC production, reaching 6.5 g BNC/L. The results demonstrate that the optimal concentration of SCOBY is considerably high, while GTI and BMJ have optimal concentrations in an intermediate range. The analysis of the center point suggests a trend toward convergence to a uniform concentration, potentially influenced by the acidic pH of the SCOBY, promoting the composition of the medium [82]. It is worth noting that BMJ possesses components abundant in sugars and nitrogenous compounds, fostering the growth of microorganisms for the production of bioproducts [25,26].

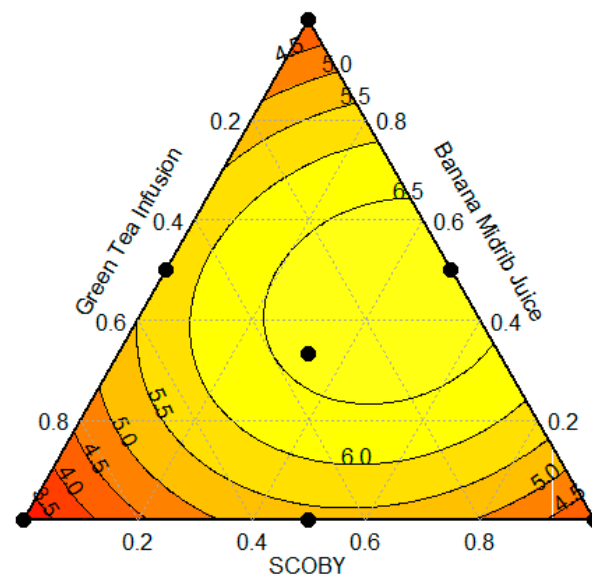


**Figure 2.** Mixing contour plot showing the effect of the variables. Colour coding makes it possible to distinguish the different yield levels of bacterial nanocellulose production: reddish tones indicate lower yields and yellow tones indicate higher yields.

### 3.3. Kinetics of BNC Production Using Optimal Values

Based on the results obtained from the simplex-centroid mixing design, production was scaled up to a 10 L bioreactor and maintained under stationary conditions at 30 °C and 1 atmosphere. Evaluations of pH, turbidity, and BNC production yield were carried out at different time intervals, specifically at 0, 4, 7, 10, and 14 days. All measurements were carried out in triplicate. See Figure 3.

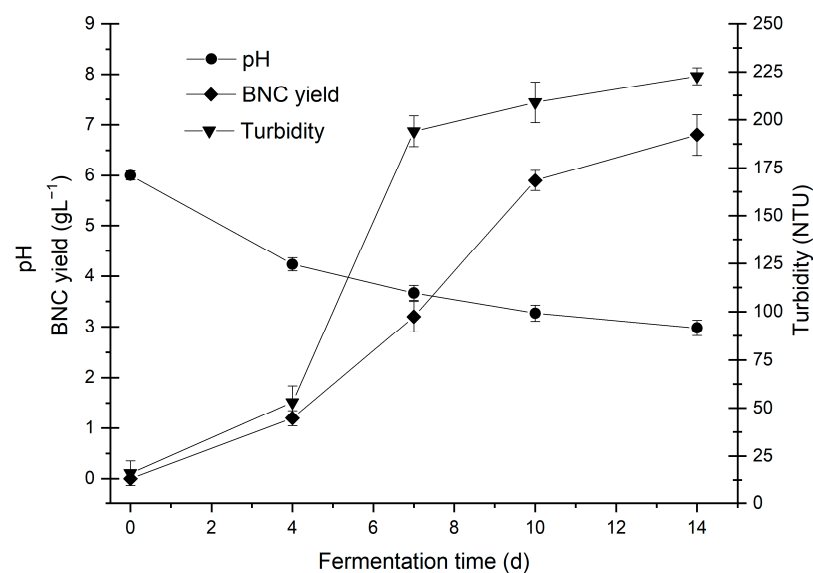


**Figure 3.** Kinetic analysis of bacterial nanocellulose production: pH and turbidity variations in the culture medium.

The results show that the pH of the culture medium decreases over time. The decrease in pH observed in kombucha tea-like fermentation media may indicate metabolic activity, as it is associated with the production of organic acids such as acetic, D-glucuronic, lactic, tartaric, and citric acids. Previous studies have suggested that these acids are generated during the fermentative process [26,83,84].

The turbidity of the optimized culture medium experienced a significant increase in the first seven days of fermentation and remained stable thereafter. During the initial phase, bacteria increase their population using oxygen, generating cellulose and turbidity. After oxygen depletion, bacteria located on the surface produce bacterial cellulose, reaching equilibrium, while those submerged in the fermentation medium become inactive below the surface. The latter can be reactivated for future cultures [83]. Regarding turbidity in kombucha analog beverages, this is associated with microbial growth. *Komagataeibacter*, predominant in the initial culture, induces cellulose production, thus exerting a direct influence on turbidity [85,86].

The formation of BNC manifested as a delicate layer, progressively thickening throughout the fermentation process, discernible from the fourth day onwards. By the 14th day, an average yield of 6.82 g BNC/L on a dry basis was attained, signifying promising outcomes. In contrast, antecedent studies reported a yield of 0.031 g/g at 21 days [26], with others achieving up to 6.4 g BNC/L of dry mass after 21 days [82]. The production of BNC from diverse raw materials, such as acerola juice extract and industrial residues, yielded 2.9 g/L after 12 days of fermentation [87]. Similarly, BNC production in black tea media recorded 3.06 g BNC/L in dry weight [88].

The utilization of banana leaf extract and green tea infusion yielded encouraging results, attributed to the richness of nutrients, vitamins, polyphenols, and phytochemicals inherent in these infusions. This strategic approach alleviated the necessity for additional nitrogen sources, consequently yielding a cost reduction [82]. Notably, this achievement can be attributed to the exploitation of symbiotic relationships among bacteria within the SCOBY. As per [89], individual strains producing BNC demonstrated a yield of 3.0–4.1%, while symbiotic cultivation achieved a BNC production ranging from 6.3% to 10.0%, underscoring a substantial enhancement in efficiency. In this context, the selection of residual biomass as a raw material not only satisfies the technical requisites for BNC production but also ensures sustainability by mitigating competition with food resources. This strategic approach presents auspicious perspectives for the proficient and cost-effective production of BNC with specialized applications.

### 3.4. Physical and Chemical Properties of Bacterial Nanocellulose

Bacterial nanocellulose was harvested from both the HS control medium (HS-BNC) and the optimized medium, which was scaled up to a volume of 10 L (SCD-BNC). Subsequently, the membranes underwent a washing process with 0.4 N NaOH, followed by rinsing with distilled water until the washing liquid achieved a neutral pH. The BNC samples were then subjected to a freeze-drying process and analyzed using SEM, FTIR, TGA, and XRD techniques to explore their physical and chemical composition.

#### 3.4.1. SEM Analysis

SEM was employed to examine the microscopic morphology of the BNC samples. Figure 4A,B illustrate the morphology of BNC produced by both the HS control medium (HS-BNC) and the SCD-optimized medium (SCD-BNC), respectively. The BNC was purified through treatment with NaOH, followed by thorough washing with water to eliminate all impurities and bacterial cells [26]. The microstructure revealed a cross-linking of cellulose fibrils in both BNC samples. The images depict the arrangement of BNCs in a layered network with randomly oriented cellulose microfibrils. In the case of HS-BNC, the diameters of the microfibrils ranged from 23.9 nm to 119.2 nm, with an average of 43.5 nm (Figure 4(C1)), consistent with previous findings [29,89]. Conversely, SCD-BNC had diameters ranging from 28.7 nm to 120.0 nm, with a mean of 58.23 nm (Figure 4(C2)). These results suggest a larger mean fiber diameter in the SCD-BNC medium, a conclusion supported by prior research focused on the evaluation of industrial waste [24,27,90]. The density, size, and arrangement of BNC fibrils depend primarily on the medium composition, viscosity, and activity of BNC-producing bacteria [27,91,92].

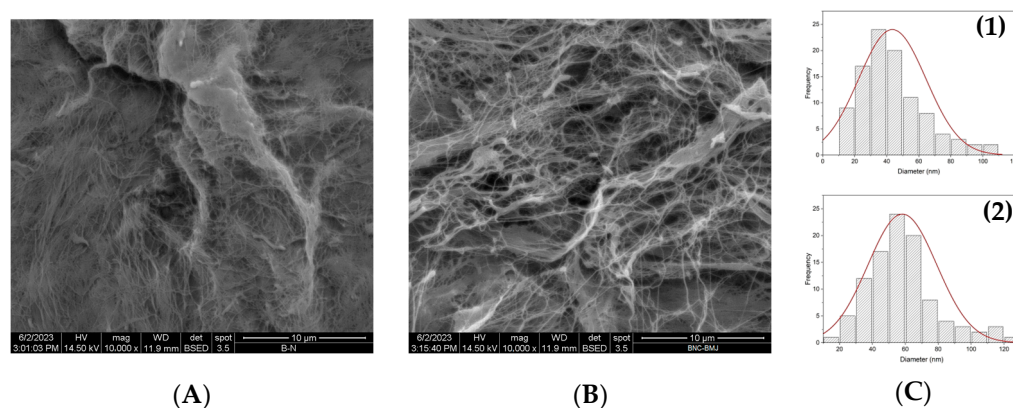


**Figure 4.** SEM images of the bacterial nanocellulose membranes: (A) Obtained in the HS control medium. (B) Obtained in the medium optimized by simplex-centroid design (SCD). Panels (C1,C2) present plots of diameter distribution and standard distribution for HS-BNC and SCD-BNC, respectively.

### 3.4.2. FTIR Analysis

The study used FT-IR analysis to evaluate the structural characteristics of HS-BNC and SCD-BNC membranes produced under different nutritional conditions. The analysis revealed characteristic bands associated with type I cellulose. Figure 5 shows similar FTIR spectra between HS-BNC and SCD-BNC, with a peak in the  $3300\text{--}3412\text{ cm}^{-1}$  region indicating the -OH stretching vibrations characteristic of type I cellulose [93,94]. Despite the similarity, there is a variation in the peak intensity for SCD-BNC in this region, indicating a modification in the hydrogen bond interaction. This alteration is attributed to both the influence of carbohydrates from the carbon source in the culture medium [87,95] and the presence of adsorbed water [96,97].

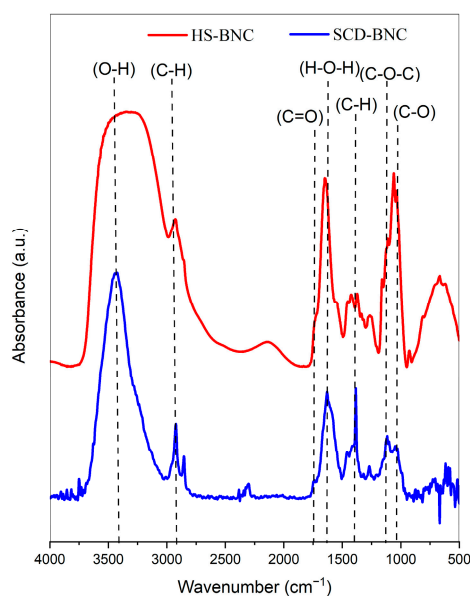


**Figure 5.** Characterization of bacterial nanocellulose: Fourier transform infrared spectroscopy spectra. The red line represents the BNC spectrum obtained in the HS control medium, whereas the blue line represents the BNC spectrum obtained in the SCD-optimized medium.

The samples also presented other relevant bands, such as those corresponding to the CH stretching of  $\text{CH}_2$  groups around  $2893\text{ cm}^{-1}$ , specific to type I cellulose [90], and the asymmetric  $\text{CH}_2$  stretching at  $2854\text{ cm}^{-1}$  [48], which represents the C-H stretching vibration of the sugar rings [27]. In the case of SCD-BNC, the simultaneous detection of both bands suggests a probable influence of the sugar substrate composition on the

fermentation process. Previous research has illustrated how different carbon sources can impact the spectrum of the BNC sample [87,98]. Additionally, prominent bands were observed around  $2250\text{ cm}^{-1}$ , corresponding to CN stretching [99], which could indicate an association with the presence of carbohydrates and nitrogenous compounds found in the ingredients used to formulate the fermentation medium [87,95,100,101]. Furthermore, an absorption band at  $1650.5\text{ cm}^{-1}$ , attributed to the presence of the carboxyl functional group (C=O), and a band around  $1642\text{ cm}^{-1}$ , attributed to H-O-H bending due to water adsorption, were observed [100,102].

The spectra of both samples showed characteristic signals of type I cellulose. Strong bands at  $1425\text{ cm}^{-1}$  were observed in the spectrum of cellulose. Strong bands at  $1425\text{ cm}^{-1}$  were assigned to  $\text{CH}_2$ - symmetric bending; a band at  $1160\text{ cm}^{-1}$  indicated C-O-C asymmetric stretching at the  $\beta$ -glycosidic bond [27,87], and a maximum at  $1068\text{ cm}^{-1}$  corresponded to C-O- symmetric stretching of the primary alcohol. The differences between SCD-BNC and HS-BNC can be attributed to the carbohydrates and phenolic compounds present in the fermentation medium. These phenolic compounds can combine with cellulose in situ during fermentation, which explains the observed changes [89,103].

### 3.4.3. TGA Analysis

The thermal stability of BNCs produced in the HS control medium (HS-BNC) and the SCD-optimized medium (SCD-BNC) was assessed through TGA, the results of which are presented in Figure 6A, and differential thermogravimetric analysis (DTG), illustrated in Figure 6B. Both BNC samples displayed similar curves with three distinct stages of mass loss. Initially, a marginal decrease in weight was observed up to approximately  $150\text{ }^\circ\text{C}$ , attributed to water evaporation during the initial heat treatment. The thermal degradation process unfolded in two discernible stages, with the second stage occurring between  $240$  and  $425\text{ }^\circ\text{C}$  and closely linked to cellulose degradation. This stage involved depolymerization, dehydration, and decomposition of the glucose units, culminating in the formation of a carbonaceous residue [104]. It resulted in a weight loss of approximately  $56.56\%$  and  $50.02\%$  in HS-BNC and SCD-BNC, respectively. The final stage, reaching  $800\text{ }^\circ\text{C}$ , showed a weight reduction of  $15.3\%$  and  $18.6\%$  in HS-BNC and SCD-BNC, respectively. Overall, the sample experienced an aggregate mass loss of  $82.09\%$  of its initial weight.

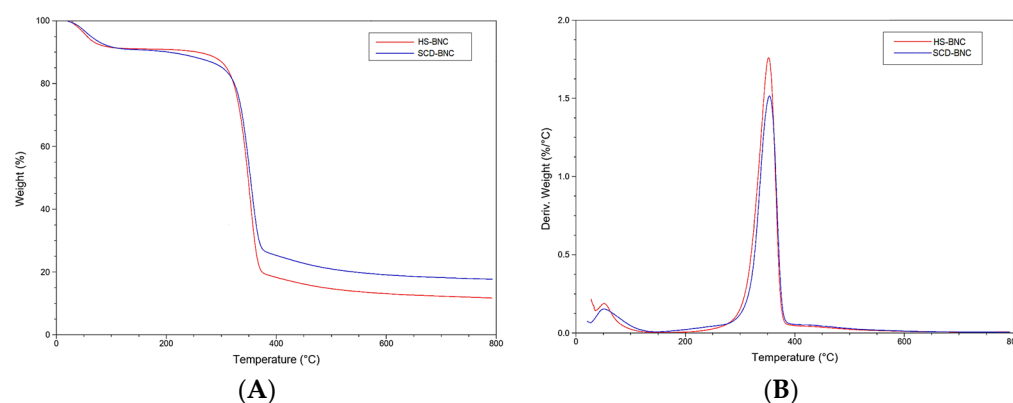


**Figure 6.** (A) Thermogravimetric analysis curve and (B) derivative thermogravimetry curve. The red line represents the BNC spectrum obtained in the HS control medium, while the blue line represents the BNC spectrum obtained in the SCD-optimized medium.

Previous studies have indicated that the mass loss of bacterial cellulose usually ranges from  $70\%$  to  $95\%$ , depending on the bacterial strain responsible for cellulose production [88,105,106]. The HS sample demonstrated a diminished residual in TGA compared to SCD, attributable to distinctions in the medium's composition and the structure of the produced BNCs [98]. In the DTG curves, the maximum decomposition temperatures ( $T_{\text{max}}$ ) for HS-BNC and SCD-BNC were  $352.24$  and  $355.51\text{ }^\circ\text{C}$ , respectively. A slight deviation in the degradation temperature could be ascribed to variations in BNC fibril size, arrange-

ment, and compactness [92]. The DTG results aligned with the XRD findings, as higher crystallinity has been reported to improve the thermal stability of BNC [107]. TGA findings for both culture media revealed similar patterns, consistent with the results of previous studies [26,29,99,108].

#### 3.4.4. XRD Analysis

BNC is a homogeneous polycrystalline macromolecular compound consisting of an ordered crystalline region and a disordered amorphous region [109]. Its remarkable crystallinity, compared to plant cellulose, serves as a distinctive attribute [29]. Within the ordered crystalline region, various BNC samples exhibit broad and robust peaks at  $2\theta = 14.5^\circ$  and  $22.7^\circ$ , values consistent with previous research [24,29,110]. The XRD patterns display three reflections at 14.5, 16.7, and 22.7, respectively. See Figure 7.

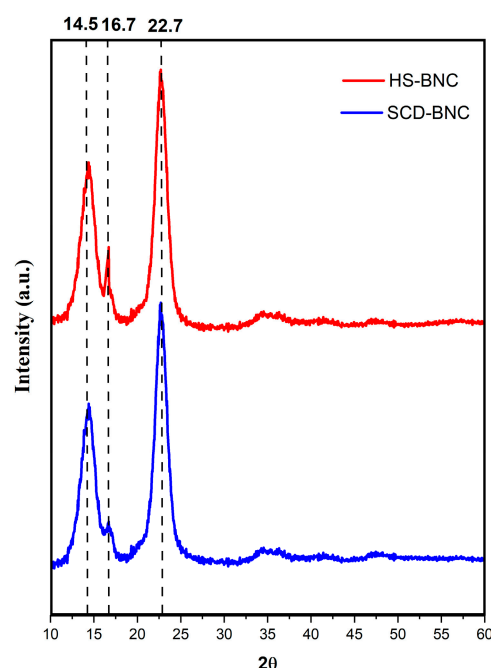


**Figure 7.** X-ray diffractogram of bacterial nanocellulose in the optimized medium from banana mid-rib juice, SCD-BNC (blue line), and bacterial nanocellulose in the HS medium, BNC (red line).

Representing typical diffraction peaks of type I cellulose and reflecting the crystalline and amorphous structure of BNC components. These results show similarities with previous studies [111,112]. The *CrI* stands as a crucial parameter for BNC and its derived compounds [113]. According to Segal's formula, the crystallinity of BNC produced in the SCD-optimized medium reached 83.5%, surpassing that of BNC produced in the HS medium (79.5%). These findings suggest that BNC from the medium optimized using BMJ has the highest cellulose I $\alpha$  content, while BNC from the HS medium has the lowest cellulose I $\alpha$  content. Various factors, such as cultivation methods, carbon sources, pH of the medium, stirring speed, temperature, cultivation time, additives, and drying methods, could influence the crystallinity of BNC [114]. The possible relationship with NaOH degradation is also considered, as this degradation process initiates the decomposition of the polymer and facilitates the hydrolysis of the cellulose [86,115].

#### 4. Conclusions

This study presents a noteworthy advancement in BNC production using sustainable resources such as BMJ and GTI. Optimization through a simplex-centroid experimental design resulted in the development of a statistically significant model, emphasizing its efficiency in compositions near the central point of the design and underscoring the industrial feasibility of utilizing agricultural by-products.

The research contributes significantly to both practical and theoretical aspects. The scalability of the process and its potential in industrial settings are demonstrated through laboratory-scale and bioreactor-scale production. A robust model has been established from a theoretical perspective, highlighting the key influence of the components of the culture medium and thus significantly contributing to the body of knowledge in this emerging field.

This study aligns with recent developments in sustainable biomaterials, emphasizing unique contributions such as the use of BMJ and GTI. It underscores the importance of utilizing renewable resources and optimizing processes to encourage further discussion on the integration of these approaches across various industrial sectors.

However, this study has inherent limitations, such as not exploring other variables. This suggests promising areas for future research, including the investigation of different biomass sources and the optimization of fermentation conditions on an industrial scale. The results demonstrate significant potential for diverse BNC applications in the industry, making a tangible contribution to both the scientific community and broader sustainable development goals.

**Author Contributions:** Conceptualization, M.F.-C., P.N.-R., J.M.B. and D.D.-L.; methodology, M.F.-C., Ó.C., R.R.-P. and D.D.-L.; software, R.R.-P., J.M.B. and M.F.-C.; validation, Ó.C., P.N.-R. and D.D.-L.; formal analysis, J.M.B., P.N.-R. and D.D.-L.; investigation, M.F.-C. and D.D.-L.; resources, R.R.-P. and Ó.C.; data curation, M.F.-C., P.N.-R., J.M.B. and D.D.-L.; writing—original draft preparation, D.D.-L.; writing—review and editing, M.F.-C. and D.D.-L.; visualization, D.D.-L.; supervision, M.F.-C.; project administration, M.F.-C.; funding acquisition, M.F.-C. and D.D.-L. All authors have read and agreed to the published version of the manuscript.

**Funding:** The APC was funded by the State University of Milagro.

**Institutional Review Board Statement:** Not applicable.

**Data Availability Statement:** Data are contained within the article.

**Acknowledgments:** The authors would like to thank Juan Tirape for his collaboration in the collection of the samples. As well as to the students, Andrés Zeas, Doménica Durán, and Anthony Tubun, for their support in the development of the experiments.

**Conflicts of Interest:** The authors declare no conflicts of interest.

## References

1. Jonas, R.; Farah, L.F. Production and application of microbial cellulose. *Polym. Degrad. Stab.* **1998**, *59*, 101–106. [[CrossRef](#)]
2. Li, W.; Zhang, S.; Zhang, T.; Shen, Y.; Han, L.; Peng, Z.; Xie, Z.; Zhong, C.; Jia, S. Bacterial cellulose production from ethylenediamine pretreated *Caragana korshinskii* Kom. In *Industrial Crops and Products*; Elsevier B.V.: Amsterdam, The Netherlands, 2021; Volume 164. [[CrossRef](#)]
3. El-Gendi, H.; Salama, A.; El-Fakharany, E.M.; Saleh, A.K. Optimization of bacterial cellulose production from prickly pear peels and its ex situ impregnation with fruit byproducts for antimicrobial and strawberry packaging applications. *Carbohydr. Polym.* **2023**, *302*, 120383. [[CrossRef](#)] [[PubMed](#)]
4. Gromovykh, T.I.; Sadykova, V.S.; Lutchenko, S.V.; Dmitrenok, A.S.; Feldman, N.B.; Danilchuk, T.N.; Kashirin, V.V. Bacterial cellulose synthesized by *Gluconacetobacter hansenii* for medical applications. *Appl. Biochem. Microbiol.* **2017**, *53*, 60–67. [[CrossRef](#)]
5. Saleh, A.K.; El-Gendi, H.; El-Fakharany, E.M.; Owda, M.E.; Awad, M.A.; Kamoun, E.A. Exploitation of cantaloupe peels for bacterial cellulose production and functionalization with green synthesized Copper oxide nanoparticles for diverse biological applications. *Sci. Rep.* **2022**, *12*, 19241. [[CrossRef](#)] [[PubMed](#)]
6. Zeng, M.; Laromaine, A.; Roig, A. Bacterial cellulose films: Influence of bacterial strain and drying route on film properties. *Cellulose* **2014**, *21*, 4455–4469. [[CrossRef](#)]
7. da Gama, F.M.P.; Dourado, F.; NanoCellulose, B. Bacterial NanoCellulose: What future? *Bioimpacts* **2018**, *8*, 1–3. [[CrossRef](#)] [[PubMed](#)]
8. Andriani, D.; Apriyana, A.Y.; Karina, M. The optimization of bacterial cellulose production and its applications: A review. *Cellulose* **2020**, *27*, 6747–6766. [[CrossRef](#)]
9. Cheng, Z.; Yang, R.; Liu, X.; Liu, X.; Chen, H. Green synthesis of bacterial cellulose via acetic acid pre-hydrolysis liquor of agricultural corn stalk used as carbon source. *Bioresour. Technol.* **2017**, *234*, 8–14. [[CrossRef](#)]
10. El-Naggar, N.E.-A.; El-Malkey, S.E.; Abu-Saied, M.A.; Mohammed, A.B.A. Exploration of a novel and efficient source for production of bacterial nanocellulose, bioprocess optimization and characterization. *Sci. Rep.* **2022**, *12*, 18533. [[CrossRef](#)]

11. Li, W.; Shen, Y.; Liu, H.; Huang, X.; Xu, B.; Zhong, C.; Jia, S. Bioconversion of lignocellulosic biomass into bacterial nanocellulose: Challenges and perspectives. *Green Chem. Eng.* **2023**, *4*, 160–172. [CrossRef]
12. Huang, Y.; Zhu, C.; Yang, J.; Nie, Y.; Chen, C.; Sun, D. Recent advances in bacterial cellulose. *Cellulose* **2014**, *21*, 1–30. [CrossRef]
13. El-Gendi, H.; Taha, T.H.; Ray, J.B.; Saleh, A.K. Recent advances in bacterial cellulose: A low-cost effective production media, optimization strategies and applications. *Cellulose* **2022**, *29*, 7495–7533. [CrossRef]
14. Azeredo, H.M.C.; Barud, H.; Farinas, C.S.; Vasconcellos, V.M.; Claro, A.M. Bacterial Cellulose as a Raw Material for Food and Food Packaging Applications. *Front. Sustain. Food Syst.* **2019**, *3*, 7. Available online: <https://www.frontiersin.org/articles/10.3389/fsufs.2019.00007> (accessed on 14 February 2024). [CrossRef]
15. Kamal, T.; Ul-Islam, M.; Fatima, A.; Ullah, M.W.; Manan, S. Cost-Effective Synthesis of Bacterial Cellulose and Its Applications in the Food and Environmental Sectors. *Gels* **2022**, *8*, 552. [CrossRef]
16. Ross, P.; Mayer, R.; Benziman, M. Cellulose biosynthesis and function in bacteria. *Microbiol. Rev.* **1991**, *55*, 35–58. [CrossRef]
17. Mujtaba, M.; Fraceto, L.F.; Fazeli, M.; Mukherjee, S.; Savassa, S.M.; de Medeiros, G.A.; Pereira, A.D.E.S.; Mancini, S.D.; Lipponen, J.; Vilaplana, F. Lignocellulosic biomass from agricultural waste to the circular economy: A review with focus on biofuels, biocomposites and bioplastics. *J. Clean. Prod.* **2023**, *402*, 136815. [CrossRef]
18. Trache, D.; Hussin, M.H.; Haafiz, M.K.M.; Thakur, V.K. Recent progress in cellulose nanocrystals: Sources and production. *Nanoscale* **2017**, *9*, 1763–1786. [CrossRef] [PubMed]
19. Rambabu, N.; Panthapulakkal, S.; Sain, M.; Dalai, A.K. Production of nanocellulose fibers from pinecone biomass: Evaluation and optimization of chemical and mechanical treatment conditions on mechanical properties of nanocellulose films. *Ind. Crops Prod.* **2016**, *83*, 746–754. [CrossRef]
20. Melikoğlu, A.Y.; Bilek, S.E.; Cesur, S. Optimum alkaline treatment parameters for the extraction of cellulose and production of cellulose nanocrystals from apple pomace. *Carbohydr. Polym.* **2019**, *215*, 330–337. [CrossRef] [PubMed]
21. Hafemann, E.; Battisti, R.; Marangoni, C.; Machado, R.A.F. Valorization of royal palm tree agroindustrial waste by isolating cellulose nanocrystals. *Carbohydr. Polym.* **2019**, *218*, 188–198. [CrossRef] [PubMed]
22. Arkell, A.; Olsson, J.; Wallberg, O. Process performance in lignin separation from softwood black liquor by membrane filtration. *Chem. Eng. Res. Des.* **2014**, *92*, 1792–1800. [CrossRef]
23. Pola, L.; Collado, S.; Oulego, P.; Díaz, M. Kraft black liquor as a renewable source of value-added chemicals. *Chem. Eng. J.* **2022**, *448*, 137728. [CrossRef]
24. Feng, X.; Ge, Z.; Wang, Y.; Xia, X.; Zhao, B.; Dong, M. Production and characterization of bacterial cellulose from kombucha-fermented soy whey. *Food Prod. Process. Nutr.* **2024**, *6*, 20. [CrossRef]
25. Tan, J.S.; Phapugrangkul, P.; Lee, C.K.; Lai, Z.-W.; Bakar, M.H.A.; Murugan, P. Banana frond juice as novel fermentation substrate for bioethanol production by *Saccharomyces cerevisiae*. *Biocatal. Agric. Biotechnol.* **2019**, *21*, 101293. [CrossRef]
26. Fiallos-Cárdenas, M.; Ramirez, A.D.; Pérez-Martínez, S.; Bonilla, H.R.; Ordoñez-Viñan, M.; Ruiz-Barzola, O.; Reinoso, M.A. Bacterial Nanocellulose Derived from Banana Leaf Extract: Yield and Variation Factors. *Resources* **2021**, *10*, 121. [CrossRef]
27. Akintunde, M.O.; Adebayo-Tayo, B.C.; Ishola, M.M.; Zamani, A.; Horváth, I.S. Bacterial Cellulose Production from agricultural Residues by two *Komagataeibacter* sp. Strains. *Bioengineered* **2022**, *13*, 10010–10025. [CrossRef] [PubMed]
28. Amorim, J.D.P.; Costa, A.F.S.; Galdino, C.J.S.; Vinhas, G.M.; Santos, E.M.S.; Sarubbo, L.A. Bacterial cellulose production using fruit residues as substrate to industrial application. *Chem. Eng. Trans.* **2019**, *74*, 1165–1170. [CrossRef]
29. Lee, J.; An, H.-E.; Lee, K.H.; Kim, S.; Park, C.; Kim, C.-B.; Yoo, H.Y. Identification of *Gluconacetobacter xylinus* LYP25 and application to bacterial cellulose production in biomass hydrolysate with acetic acid. *Int. J. Biol. Macromol.* **2024**, *261*, 129597. [CrossRef] [PubMed]
30. Anguluri, K.; La China, S.; Bruognoli, M.; Cassanelli, S.; Gullo, M. Better under stress: Improving bacterial cellulose production by *Komagataeibacter xylinus* K2G30 (UMCC 2756) using adaptive laboratory evolution. *Front. Microbiol.* **2022**, *13*, 994097. [CrossRef] [PubMed]
31. Anusuya, R.S.; Anandham, R.; Kumutha, K.; Gayathry, G.; Mageshwaran, V.; Uthandi, S. Characterization and optimization of bacterial cellulose produced by *Acetobacter* spp. *J. Environ. Biol.* **2020**, *41*, 207–215. [CrossRef]
32. Wang, X.; Zhong, J.-J. Improvement of bacterial cellulose fermentation by metabolic perturbation with mixed carbon sources. *Process Biochem.* **2022**, *122*, 95–102. [CrossRef]
33. Chandana, A.; Mallick, S.P.; Dikshit, P.K.; Singh, B.N.; Sahi, A.K. Recent Developments in Bacterial Nanocellulose Production and its Biomedical Applications. *J. Polym. Environ.* **2022**, *30*, 4040–4067. [CrossRef]
34. Öztürk, B.E.T.; Eroğlu, B.; Delik, E.; Çiçek, M.; Çiçek, E. Comprehensive Evaluation of Three Important Herbs for Kombucha Fermentation. *Food Technol. Biotechnol.* **2023**, *61*, 127–137. [CrossRef] [PubMed]
35. Hata, N.N.Y.; Surek, M.; Sartori, D.; Serrato, R.V.; Spinosa, W.A. Role of Acetic Acid Bacteria in Food and Beverages. *Food Technol. Biotechnol.* **2023**, *61*, 85–103. [CrossRef]
36. Halib, N.; Amin, M.C.I.M. Physicochemical Properties and Characterization of Nata de Coco from Local Food Industries as a Source of Cellulose. Sifat Fizikokimia dan Pencirian Nata de Coco daripada Industri Makanan Tempatan Sebagai Sumber Selulosa. 2012. Available online: [https://www.ukm.my/jsm/pdf\\_files/SM-PDF-41-2-2012/08%20Nadia.pdf](https://www.ukm.my/jsm/pdf_files/SM-PDF-41-2-2012/08%20Nadia.pdf) (accessed on 30 July 2023).
37. Zhang, J.; Yang, Y.; Deng, J.; Wang, Y.; Hu, Q.; Li, C.; Liu, S. Dynamic profile of the microbiota during coconut water pre-fermentation for nata de coco production. *LWT-Food Sci. Technol.* **2017**, *81*, 87–93. [CrossRef]

38. Devi, A.; Bajar, S.; Kour, H.; Kothari, R.; Pant, D.; Singh, A. Lignocellulosic Biomass Valorization for Bioethanol Production: A Circular Bioeconomy Approach. *BioEnergy Res.* **2022**, *15*, 1820–1841. [[CrossRef](#)] [[PubMed](#)]
39. Liu, X.; Ding, S.; Gao, F.; Wang, Y.; Taherzadeh, M.J.; Wang, Y.; Qin, X.; Wang, X.; Luo, H.; Yao, B.; et al. Exploring the cellulolytic and hemicellulolytic activities of manganese peroxidase for lignocellulose deconstruction. *Biotechnol. Biofuels Bioprod.* **2023**, *16*, 139. [[CrossRef](#)] [[PubMed](#)]
40. Singh, N.; Singhania, R.R.; Nigam, P.S.; Dong, C.-D.; Patel, A.K.; Puri, M. Global status of lignocellulosic biorefinery: Challenges and perspectives. *Bioresour. Technol.* **2022**, *344*, 126415. [[CrossRef](#)]
41. Chaityachet, O.A.; Thongmoon, S.; Udomchai, T. Utilization of Yam Bean Juice as Nutrient Source for Bacterial Cellulose Production by *Komagataeibacter nataicola* TISTR 975. *Curr. Nutr. Food Sci.* **2023**, *19*, 564–571. [[CrossRef](#)]
42. Coton, M.; Pawtowski, A.; Taminiau, B.; Burgaud, G.; Deniel, F.; Coulloume-Labarthe, L.; Fall, A.; Daube, G.; Coton, E. Unraveling microbial ecology of industrial-scale Kombucha fermentations by metabarcoding and culture-based methods. *FEMS Microbiol. Ecol.* **2017**, *93*, fix048. [[CrossRef](#)]
43. Hestrin, S.; Schramm, M. Synthesis of cellulose by *Acetobacter xylinum*. II. Preparation of freeze-dried cells capable of polymerizing glucose to cellulose. *Biochem. J.* **1954**, *58*, 345–352. [[CrossRef](#)] [[PubMed](#)]
44. Kaewkod, T.; Sangboonruang, S.; Khacha-Ananda, S.; Charoenrak, S.; Bovonsombut, S.; Tragoolpua, Y. Combinations of traditional kombucha tea with medicinal plant extracts for enhancement of beneficial substances and activation of apoptosis signaling pathways in colorectal cancer cells. *Food Sci. Technol. Braz.* **2022**, *42*, e107521. [[CrossRef](#)]
45. Neves, E.Z.; Kumineck Junior, S.R.; Katrucha, G.P.; Silveira, V.F.; Silveira ML, L.; Pezzin AP, T.; dos Santos Schneider, A.L.; Garcia MC, F.; Apati, G.P. Development of Bacterial Cellulose Membranes Incorporated with Plant Extracts. *Macromol. Symp.* **2022**, *406*, 2200031. [[CrossRef](#)]
46. Sharma, C.; Bhardwaj, N.K. Bacterial nanocellulose: Present status, biomedical applications and future perspectives. *Mater. Sci. Eng. C* **2019**, *104*, 109963. [[CrossRef](#)]
47. Bekatorou, A.; Plioni, I.; Sparou, K.; Maroutsiou, R.; Tsafrakidou, P.; Petsi, T.; Kordouli, E. Bacterial Cellulose Production Using the Corinthian Currant Finishing Side-Stream and Cheese Whey: Process Optimization and Textural Characterization. *Foods* **2019**, *8*, 193. [[CrossRef](#)]
48. Cerrutti, P.; Roldán, P.; García, R.M.; Galvagno, M.A.; Vázquez, A.; Foresti, M.L. Production of bacterial nanocellulose from wine industry residues: Importance of fermentation time on pellicle characteristics. *J. Appl. Polym. Sci.* **2016**, *133*, 14. [[CrossRef](#)]
49. Öz, Y.E.; Kalender, M. Optimization Of Bacterial Cellulose Production From Sugar Beet Molasses By *Gluconacetobacter Xylinus* Nrrl B-759 In Static Culture. *Cellul. Chem. Technol.* **2021**, *55*, 1051–1060. [[CrossRef](#)]
50. Rodrigues, A.C.; Fontão, A.I.; Coelho, A.; Leal, M.; da Silva, F.A.S.; Wan, Y.; Dourado, F.; Gama, M. Response surface statistical optimization of bacterial nanocellulose fermentation in static culture using a low-cost medium. *New Biotechnol.* **2019**, *49*, 19–27. [[CrossRef](#)]
51. Liu, C.; Wang, X.; Yang, H.; Liu, C.; Zhang, Z.; Chen, G. Biodegradable polyhydroxyalkanoates production from wheat straw by recombinant *Halomonas elongata* A1. *Int. J. Biol. Macromol.* **2021**, *187*, 675–682. [[CrossRef](#)]
52. Gómez-García, R.; Campos, D.A.; Aguilar, C.N.; Madureira, A.R.; Pintado, M. Valorisation of food agro-industrial by-products: From the past to the present and perspectives. *J. Environ. Manag.* **2021**, *299*, 113571. [[CrossRef](#)]
53. Galvan, D.; Eftting, L.; Cremasco, H.; Conte-Junior, C.A. Recent Applications of Mixture Designs in Beverages, Foods, and Pharmaceutical Health: A Systematic Review and Meta-Analysis. *Foods* **2021**, *10*, 1941. [[CrossRef](#)]
54. Lawson, J.; Willden, C. Mixture Experiments in R Using mixexp. *J. Stat. Softw.* **2016**, *72*, 1–20. [[CrossRef](#)]
55. Cini, J.R.D.M.; Borsato, D.; Guedes, C.L.B.; da Silva, H.C.; Coppo, R.L. Comparison of methods for determination of oxidative stability of B100 biodiesel mixed with synthetic antioxidants: Application of simplex-centroid design with process variable. *Quím. Nova* **2013**, *36*, 79–84. [[CrossRef](#)]
56. Correia, I.; Borsato, D.; Savada, F.; Pauli, E.; Mantovani, A.; Cremasco, H.; Chendynski, L. Inhibition of the biodiesel oxidation by alcoholic extracts of green and black tea leaves and plum pulp: Application of the simplex-centroid design. *Renew. Energy* **2020**, *160*, 288–296. [[CrossRef](#)]
57. Pauli, E.D.; Malta, G.B.; Sanchez, P.M.; Moreira, I.C.; Scarminio, I.S. Mixture design analysis of solvent extractor effects on epicatechin, epigallocatechin gallate, epigallocatechin and antioxidant activities of the *Camellia sinensis* L. leaves. *Anal. Chem. Res.* **2014**, *2*, 23–29. [[CrossRef](#)]
58. Squeo, G.; De Angelis, D.; Leardi, R.; Summo, C.; Caponio, F. Background, Applications and Issues of the Experimental Designs for Mixture in the Food Sector. *Foods* **2021**, *10*, 1128. [[CrossRef](#)] [[PubMed](#)]
59. Cornell, J.A. *A Primer on Experiments with Mixtures*; John Wiley & Sons: Hoboken, NJ, USA, 2011; p. 351. [[CrossRef](#)]
60. Filho, R.C.N.; Galvan, D.; Eftting, L.; Terhaag, M.M.; Yamashita, F.; Benassi, M.D.T.; Spinosa, W.A. Effects of adding spices with antioxidants compounds in red ale style craft beer: A simplex-centroid mixture design approach. *Food Chem.* **2021**, *365*, 130478. [[CrossRef](#)] [[PubMed](#)]
61. Rahman, M.A.; Saha, C.K.; Ward, A.J.; Møller, H.B.; Alam, M.M. Anaerobic co-digestions of agro-industrial waste blends using mixture design. *Biomass Bioenergy* **2019**, *122*, 156–164. [[CrossRef](#)]
62. Wang, P.; Li, X.; Huo, X.; Ali, S.; Sun, J.; Qin, J.; Liang, K.; Liu, Y. Early hydration and compressive strength of steam cured high-strength concrete based on simplex centroid design method. *Case Stud. Constr. Mater.* **2022**, *17*, e01583. [[CrossRef](#)]

63. Chen, Y.; Liu, P.; Sha, F.; He, S.; Lu, G.; Yu, Z.; Chen, H. Preparation and performance of the ultra-high performance mortar based on simplex-centroid design method. *J. Mater. Res. Technol.* **2021**, *15*, 3060–3077. [[CrossRef](#)]
64. Jiao, D.; Shi, C.; Yuan, Q.; An, X.; Liu, Y. Mixture design of concrete using simplex centroid design method. *Cem. Concr. Compos.* **2018**, *89*, 76–88. [[CrossRef](#)]
65. Miller, G.L. Use of Dinitrosalicylic Acid Reagent for Determination of Reducing Sugar. ACS Publications. Available online: <https://pubs.acs.org/doi/pdf/10.1021/ac60147a030> (accessed on 14 November 2023).
66. Liu, X.; Cao, L.; Wang, S.; Huang, L.; Zhang, Y.; Tian, M.; Li, X.; Zhang, J. Isolation and characterization of bacterial cellulose produced from soybean whey and soybean hydrolyzate. *Sci. Rep.* **2023**, *13*, 16024. [[CrossRef](#)] [[PubMed](#)]
67. Segal, L.; Creely, J.J.; Martin, A.E.; Conrad, C.M. An Empirical Method for Estimating the Degree of Crystallinity of Native Cellulose Using the X-Ray Diffractometer. *Text. Res. J.* **1959**, *29*, 786–794. [[CrossRef](#)]
68. Ma, T.; Zhao, Q.Q.; Ji, K.H.; Zeng, B.; Li, G.Q. Homogeneous and porous modified bacterial cellulose achieved by in situ modification with low amounts of carboxymethyl cellulose. *Cellulose* **2014**, *21*, 2637–2646. [[CrossRef](#)]
69. Mago, M.; Yadav, A.; Gupta, R.; Garg, V.K. Management of banana crop waste biomass using vermicomposting technology. *Bioresour. Technol.* **2021**, *326*, 124742. [[CrossRef](#)]
70. Fiallos-Cárdenas, M.; Pérez-Martínez, S.; Ramirez, A.D. Prospectives for the development of a circular bioeconomy around the banana value chain. *Sustain. Prod. Consum.* **2022**, *30*, 541–555. [[CrossRef](#)]
71. Bai, F.; Chen, G.; Niu, H.; Zhu, H.; Huang, Y.; Zhao, M.; Hou, R.; Peng, C.; Li, H.; Wan, X.; et al. The types of brewing water affect tea infusion flavor by changing the tea mineral dissolution. *Food Chem. X* **2023**, *18*, 100681. [[CrossRef](#)] [[PubMed](#)]
72. Kim, Y.; Lee, K.-G.; Kim, M.K. Volatile and non-volatile compounds in green tea affected in harvesting time and their correlation to consumer preference. *J. Food Sci. Technol.* **2016**, *53*, 3735–3743. [[CrossRef](#)] [[PubMed](#)]
73. Tan, H.-L.; Ojukwu, M.; Lee, L.-X.; Easa, A.M. Quality characteristics of green Tea's infusion as influenced by brands and types of brewing water. *Heliyon* **2023**, *9*, 2. [[CrossRef](#)]
74. Costa, M.A.D.C.; Moreira, L.D.P.D.; Duarte, V.D.S.; Cardoso, R.R.; José, V.P.B.D.S.; da Silva, B.P.; Grancieri, M.; Corich, V.; Giacomini, A.; Bressan, J.; et al. Kombuchas from Green and Black Tea Modulate the Gut Microbiota and Improve the Intestinal Health of Wistar Rats Fed a High-Fat High-Fructose Diet. *Nutrients* **2022**, *14*, 5234. [[CrossRef](#)]
75. Ulusoy, A.; Tamer, C.E. Determination of suitability of black carrot (*Daucus carota* L. spp. *sativus* var. *atrorubens* Alef.) juice concentrate, cherry laurel (*Prunus laurocerasus*), blackthorn (*Prunus spinosa*) and red raspberry (*Rubus idaeus*) for kombucha beverage production. *J. Food Meas. Charact.* **2019**, *13*, 1524–1536. [[CrossRef](#)]
76. He, Y.; Yang, Y.; Lin, Q.; Jin, T.; Zang, X.; Yun, T.; Ding, Z.; Rekaby, S.A.; Zhao, Z.; Eissa, M.A. Physio-biochemical evaluation of Si-rich biochar amendment to improve the salt stress tolerance of Grand Nain and Williams banana genotypes. *Ind. Crops Prod.* **2023**, *204*, 117333. [[CrossRef](#)]
77. Walker, G.M.; Stewart, G.G. *Saccharomyces cerevisiae* in the Production of Fermented Beverages. *Beverages* **2016**, *2*, 30. [[CrossRef](#)]
78. Marie-Magdeleine, C.; Boval, M.; Philibert, L.; Borde, A.; Archimède, H. Effect of banana foliage (*Musa x paradisiaca*) on nutrition, parasite infection and growth of lambs. *Livest. Sci.* **2010**, *131*, 234–239. [[CrossRef](#)]
79. Lucaciu, L.A.; Seicean, R.; Seicean, A. Small molecule drugs in the treatment of inflammatory bowel diseases: Which one, when and why?—A systematic review. *Eur. J. Gastroenterol. Hepatol.* **2020**, *32*, 669–677. [[CrossRef](#)] [[PubMed](#)]
80. Nurcholis, W.; Marliani, N.; Asyhar, R.; Minarni, M. Optimized Solvents for the Maceration of Phenolic Antioxidants from *Curcuma xanthorrhiza* Rhizome using a Simplex Centroid Design. *J. Pharm. Bioallied Sci.* **2023**, *15*, 35. [[CrossRef](#)]
81. Laavanya, D.; Shirkole, S.; Balasubramanian, P. Current challenges, applications and future perspectives of SCOBY cellulose of Kombucha fermentation. *J. Clean. Prod.* **2021**, *295*, 126454. [[CrossRef](#)]
82. Dartora, B.; Hickert, L.R.; Fabricio, M.F.; Ayub, M.A.Z.; Furlan, J.M.; Wagner, R.; Perez, K.J.; Sant'Anna, V. Understanding the effect of fermentation time on physicochemical characteristics, sensory attributes, and volatile compounds in green tea kombucha. *Food Res. Int.* **2023**, *174*, 113569. [[CrossRef](#)]
83. Manan, S.; Ullah, M.W.; Ul-Islam, M.; Shi, Z.; Gauthier, M.; Yang, G. Bacterial cellulose: Molecular regulation of biosynthesis, supramolecular assembly, and tailored structural and functional properties. *Prog. Mater. Sci.* **2022**, *129*, 100972. [[CrossRef](#)]
84. Aditiawati, P.; Taufik, I.; Alexis, J.J.G.; Dungani, R. Bacterial Nanocellulose from Symbiotic Culture of Bacteria and Yeast Kombucha Prepared with Lemongrass Tea and Sucrose: Optimization and Characterization. *BioResources* **2023**, *18*, 3178–3197. [[CrossRef](#)]
85. Hatiboruah, D.; Devi, D.Y.; Namsa, N.D.; Nath, P. Turbidimetric analysis of growth kinetics of bacteria in the laboratory environment using smartphone. *J. Biophotonics* **2020**, *13*, e201960159. [[CrossRef](#)] [[PubMed](#)]
86. Leonarski, E.; Cesca, K.; Borges, O.M.A.; de Oliveira, D.; Poletto, P. Typical kombucha fermentation: Kinetic evaluation of beverage and morphological characterization of bacterial cellulose. *J. Food Process. Preserv.* **2021**, *45*, e16100. [[CrossRef](#)]
87. Hamed, D.A.; Maghrawy, H.H.; Kareem, H.A. Biosynthesis of bacterial cellulose nanofibrils in black tea media by a symbiotic culture of bacteria and yeast isolated from commercial kombucha beverage. *World J. Microbiol. Biotechnol.* **2022**, *39*, 48. [[CrossRef](#)] [[PubMed](#)]
88. Skiba, E.A.; Shavyrkina, N.A.; Skiba, M.A.; Mironova, G.F.; Budaeva, V.V. Biosynthesis of Bacterial Nanocellulose from Low-Cost Cellulosic Feedstocks: Effect of Microbial Producer. *Int. J. Mol. Sci.* **2023**, *24*, 14401. [[CrossRef](#)] [[PubMed](#)]

89. Li, Z.-Y.; Azi, F.; Ge, Z.-W.; Liu, Y.-F.; Yin, X.-T.; Dong, M.-S. Bio-conversion of kitchen waste into bacterial cellulose using a new multiple carbon utilizing *Komagataeibacter rhaeticus*: Fermentation profiles and genome-wide analysis. *Int. J. Biol. Macromol.* **2021**, *191*, 211–221. [[CrossRef](#)] [[PubMed](#)]
90. Khattak, W.A.; Khan, T.; Ul-Islam, M.; Wahid, F.; Park, J.K. Production, Characterization and Physico-mechanical Properties of Bacterial Cellulose from Industrial Wastes. *J. Polym. Environ.* **2015**, *23*, 45–53. [[CrossRef](#)]
91. Khattak, W.A.; Khan, T.; Ul-Islam, M.; Wahid, F.; Park, J.K. Production, characterization and biological features of bacterial cellulose from scum obtained during preparation of sugarcane jaggery (gur). *J. Food Sci. Technol.* **2015**, *52*, 8343–8349. [[CrossRef](#)] [[PubMed](#)]
92. Ul-Islam, M.; Khan, T.; Park, J.K. Water holding and release properties of bacterial cellulose obtained by in situ and ex situ modification. *Carbohydr. Polym.* **2012**, *88*, 596–603. [[CrossRef](#)]
93. Pacheco, G.; Nogueira, C.R.; Meneguín, A.B.; Trovatti, E.; Silva, M.C.C.; Machado, R.T.A.; Ribeiro, S.J.L.; da Silva Filho, E.C.; Barud, H.D.S. Development and characterization of bacterial cellulose produced by cashew tree residues as alternative carbon source. *Ind. Crops Prod.* **2017**, *107*, 13–19. [[CrossRef](#)]
94. Taokaew, S.; Seetabhawang, S.; Siripong, P.; Phisalaphong, M. Biosynthesis and Characterization of Nanocellulose-Gelatin Films. *Materials* **2013**, *6*, 782. [[CrossRef](#)]
95. Ghozali, M.; Meliana, Y.; Masruchin, N.; Rusmana, D.; Chalid, M. Preparation and characterization of *Arenga pinnata* thermoplastic starch/bacterial cellulose nanofiber biocomposites via *in-situ* twin screw extrusion. *Int. J. Biol. Macromol.* **2024**, *261*, 129792. [[CrossRef](#)] [[PubMed](#)]
96. El-Shall, F.N.; Al-Shemy, M.T.; Dawwam, G.E. Multifunction smart nanocomposite film for food packaging based on carboxymethyl cellulose/Kombucha SCOBY/pomegranate anthocyanin pigment. *Int. J. Biol. Macromol.* **2023**, *242*, 125101. [[CrossRef](#)]
97. Fatima, A.; Yasir, S.; Ul-Islam, M.; Kamal, T.; Ahmad, W.; Abbas, Y.; Manan, S.; Ullah, M.W.; Yang, G. Ex situ development and characterization of green antibacterial bacterial cellulose-based composites for potential biomedical applications. *Adv. Compos. Hybrid Mater.* **2022**, *5*, 307–321. [[CrossRef](#)]
98. Thorat, M.N.; Dastager, S.G. High yield production of cellulose by a: *Komagataeibacter rhaeticus* PG2 strain isolated from pomegranate as a new host. *RSC Adv.* **2018**, *8*, 29797–29805. [[CrossRef](#)] [[PubMed](#)]
99. Jiamsawat, C.; Wasanapiarnpong, T.; Srikulkit, K. Improving carbon yield of bacterial cellulose derived carbon by phosphorus/nitrogen doping. *Mater. Today Commun.* **2022**, *33*, 104382. [[CrossRef](#)]
100. Nguyen, H.T.; Saha, N.; Ngwabebhoh, F.A.; Zandraa, O.; Saha, T.; Saha, P. Kombucha-derived bacterial cellulose from diverse wastes: A prudent leather alternative. *Cellulose* **2021**, *28*, 9335–9353. [[CrossRef](#)]
101. Pereira, E.H.D.S.; Attallah, O.A.; Tas, C.E.; Chee, B.S.; Freitas, F.; Garcia, E.L.; Mc Auliffe, M.A.; Mojicevic, M.; Batista, M.N.; Reis, M.A.; et al. Boosting bacterial nanocellulose production from chemically recycled post-consumer polyethylene terephthalate. *Sustain. Mater. Technol.* **2024**, *39*, e00784. [[CrossRef](#)]
102. Amin, M.Z.; Islam, T.; Mostofa, F.; Uddin, M.J.; Rahman, M.M.; Satter, M.A. Comparative assessment of the physicochemical and biochemical properties of native and hybrid varieties of pumpkin seed and seed oil (*Cucurbita maxima* Linn.). *Heliyon* **2019**, *5*, e02994. [[CrossRef](#)]
103. Phan, A.D.T.; Flanagan, B.M.; D’Arcy, B.R.; Gidley, M.J. Binding selectivity of dietary polyphenols to different plant cell wall components: Quantification and mechanism. *Food Chem.* **2017**, *233*, 216–227. [[CrossRef](#)]
104. Öz, Y.E.; Kalender, M. A novel static cultivation of bacterial cellulose production from sugar beet molasses: Series static culture (SSC) system. *Int. J. Biol. Macromol.* **2023**, *225*, 1306–1314. [[CrossRef](#)]
105. Machado, R.T.; Meneguín, A.B.; Sábio, R.M.; Franco, D.F.; Antonio, S.G.; Gutierrez, J.; Tercjak, A.; Berretta, A.A.; Ribeiro, S.J.; Lazarini, S.C.; et al. *Komagataeibacter rhaeticus* grown in sugarcane molasses-supplemented culture medium as a strategy for enhancing bacterial cellulose production. *Ind. Crops Prod.* **2018**, *122*, 637–646. [[CrossRef](#)]
106. Lin, S.-P.; Huang, Y.-H.; Hsu, K.-D.; Lai, Y.-J.; Chen, Y.-K.; Cheng, K.-C. Isolation and identification of cellulose-producing strain *Komagataeibacter intermedius* from fermented fruit juice. *Carbohydr. Polym.* **2016**, *151*, 827–833. [[CrossRef](#)]
107. Naeem, M.A.; Siddiqui, Q.; Khan, M.R.; Mushtaq, M.; Wasim, M.; Farooq, A.; Naveed, T.; Wei, Q. Bacterial cellulose-natural fiber composites produced by fibers extracted from banana peel waste. *J. Ind. Text.* **2022**, *51*, 990S–1006S. [[CrossRef](#)]
108. Yang, L.; Zhu, X.; Chen, Y.; Wang, J. Enhanced bacterial cellulose production in *Gluconacetobacter xylinus* by overexpression of two genes (*bscC* and *bscD*) and a modified static culture. *Int. J. Biol. Macromol.* **2024**, *260*, 129552. [[CrossRef](#)]
109. French, A.D. Idealized powder diffraction patterns for cellulose polymorphs. *Cellulose* **2014**, *21*, 885–896. [[CrossRef](#)]
110. Fan, X.; Gao, Y.; He, W.; Hu, H.; Tian, M.; Wang, K.; Pan, S. Production of nano bacterial cellulose from beverage industrial waste of citrus peel and pomace using *Komagataeibacter xylinus*. *Carbohydr. Polym.* **2016**, *151*, 1068–1072. [[CrossRef](#)] [[PubMed](#)]
111. Du, R.; Zhao, F.; Peng, Q.; Zhou, Z.; Han, Y. Production and characterization of bacterial cellulose produced by *Gluconacetobacter xylinus* isolated from Chinese persimmon vinegar. *Carbohydr. Polym.* **2018**, *194*, 200–207. [[CrossRef](#)]
112. Gomes, F.P.; Silva, N.H.C.S.; Trovatti, E.; Serafim, L.S.; Duarte, M.F.; Silvestre, A.J.D.; Neto, C.P.; Freire, C.S.R. Production of bacterial cellulose by *Gluconacetobacter sacchari* using dry olive mill residue. *Biomass Bioenergy* **2013**, *55*, 205–211. [[CrossRef](#)]
113. French, A.D.; Cintrón, M.S. Cellulose polymorphy, crystallite size, and the Segal Crystallinity Index. *Cellulose* **2013**, *20*, 583–588. [[CrossRef](#)]

114. Jung, H.-I.; Lee, O.-M.; Jeong, J.-H.; Jeon, Y.-D.; Park, K.-H.; Kim, H.-S.; An, W.-G.; Son, H.-J. Production and Characterization of Cellulose by *Acetobacter* sp. V6 Using a Cost-Effective Molasses–Corn Steep Liquor Medium. *Appl. Biochem. Biotechnol.* **2010**, *162*, 486–497. [[CrossRef](#)]
115. Leonarski, E.; Martini, G.V.; Cesca, K.; SILVA, M.F.D.A.; Goldbeck, R.; Poletto, P. Enzymatic upcycling of bacterial cellulose from kombucha to obtain cellobiose. *Cellul. Chem. Technol.* **2023**, *57*, 125–132. [[CrossRef](#)]

**Disclaimer/Publisher’s Note:** The statements, opinions and data contained in all publications are solely those of the individual author(s) and contributor(s) and not of MDPI and/or the editor(s). MDPI and/or the editor(s) disclaim responsibility for any injury to people or property resulting from any ideas, methods, instructions or products referred to in the content.